

Resonant tunneling in a transverse magnetic field: Transition from the electric to the magnetic quantum limit

M. Helm, F. M. Peeters,* P. England, J. R. Hayes, and E. Colas

Bellcore, Red Bank, New Jersey 07701-7040

(Received 14 November 1988)

Resonant tunneling of electrons through a wide quantum well is quenched in a strong transverse magnetic field. In weak magnetic fields the resonances in the current weaken and shift, while in strong magnetic fields these quantum-well resonances disappear and a new series of resonances appears at low bias. We show that these new resonances correspond to states which are bound to the first barrier and have comparable amplitude on either side of the barrier. Good agreement is found with a numerical solution of the Schrödinger equation in the barrier region.

Advances in modern epitaxial-crystal-growth techniques have enabled researchers to engineer the band structure of semiconductors so that charge carriers can be forced to move in tailored potentials. This design freedom allows one to study basic quantum-mechanical problems, can lead to the discovery of new physical phenomena, and can have useful application in novel devices. One of the most widely investigated structures is the double-barrier resonant-tunneling diode,¹ which consists of two potential barriers separated by a well region. By biasing the structure electrons can tunnel through one barrier into the well and leave the structure by tunneling through the other barrier. Whenever the conduction band of the injector is lined up with a bound state of the well, a peak in the current is observed. By changing the bias continuously a number of peaks in the current-voltage characteristics can be seen, depending to first order on the well width.²⁻⁴ It has been demonstrated that the application of a magnetic field parallel to the current flow (perpendicular to the layers) results in conductance oscillations revealing the formation of Landau levels in the quantum well.⁵ The application of a magnetic field parallel to the two-dimensional layer in a quantum well leads to the formation of combined electric-magnetic subbands.⁶ As long as the magnetic field is weak, so that the cyclotron energy is smaller than the ground-state energy of the electrons in the well, it only acts as a perturbation, slightly increasing the energy of the bound states. When the magnetic field becomes larger and the cyclotron energy comparable to the electric ground-state energy, the states change from electric type to magnetic type. The energy levels are then dependent on the position of the electron in the well with respect to the barriers. At the well center the levels are equally spaced by $\hbar\omega_c$ as would be expected for bulk Landau levels; at the edges, however, the energy increases due to the presence of the barriers. Transport through such structures in a transverse magnetic field has only recently been studied.⁷⁻¹² A rigorous treatment of this configuration shows that current flow in the electric field direction is only possible if scattering is included, which implies that transport becomes diffusive rather than ballistic.

Recently, Davies *et al.*⁸ and Leadbeater *et al.*⁹ have investigated resonant tunneling in a transverse magnetic field. They found a shift of the resonances to higher volt-

ages as well as a suppression of the conductivity at low bias. These effects could be explained by considering the conservation of canonical momentum upon tunneling, which can be classically interpreted as the transfer of transverse momentum due to the Lorentz force. In addition, Snell *et al.*¹⁰ have studied tunneling through a single barrier and found oscillations in the second derivative of the current with respect to the magnetic field. In the frame of a WKB approximation, they interpreted these results as evidence for skipping orbits along the barrier. Transverse magnetotunneling has also been investigated theoretically very recently.^{13,14}

In this Rapid Communication we report the investigation of resonant tunneling in a structure that has a relatively wide GaAs quantum-well region. At zero magnetic field we observe six current peaks as a function of applied voltage, stemming from resonant tunneling into the two-dimensional electric subbands of the well. Upon increasing the magnetic field these resonances become weaker and shift to higher voltages. At very high magnetic fields a new series of resonances appears, which, as we will show, correspond to the anticrossing points of the energy levels on the left- and right-hand side of the first barrier. These resonances are not influenced by the second barrier and can be considered classically as barrier skipping orbits. Quantum mechanically they are the states which have a high probability amplitude on both sides of the barrier. The correspondence is shown by a numerical solution of the Schrödinger equation for the barrier under bias. Hence, the variation of the magnetic field and the bias voltage allows one to tune the system from electrically quantized behavior (resonant tunneling, ballistic transport) to magnetically quantized behavior (barrier bound resonances, diffusive transport).

The sample was grown by organometallic chemical vapor deposition (OMCVD) on an n^+ (100)-oriented GaAs substrate. On top of the n^+ GaAs buffer layer was grown a 330-Å-wide undoped GaAs well sandwiched between two undoped 130-Å-thick $\text{Al}_{0.3}\text{Ga}_{0.7}\text{As}$ barriers. A 1500-Å-wide region of nominally $7 \times 10^{16} \text{ cm}^{-3}$ n -type doping was grown on the top barrier followed by an n^+ region to facilitate Ohmic contact formation. The structure was fabricated into 200- μm -diam mesas using standard chemical etching techniques. Ohmic contacts were made to the

top and bottom n^+ layers by alloying an evaporated Au-Sn alloy.

Figure 1 shows the current-voltage characteristics of the resonant tunnel diode in zero magnetic field at 6 K. Six resonances are clearly observed (four of them have an associated negative differential resistance), corresponding to resonant tunneling into the six lowest subbands of the quantum well (denoted E_n). No resonances are observed in the other polarity because of the high doping adjacent to the second barrier.

Figure 2 shows the second derivative of the current with respect to the voltage, d^2I/dV^2 , for different magnetic field values. At 8 T the resonant structure has weakened and shifted to higher bias voltage. (Minima in d^2I/dV^2 correspond to maxima in the I - V characteristics.) The same effect has been reported by other groups^{8,9} and explained by the transverse momentum transfer of eBd , where d is the barrier thickness, upon tunneling due to the Lorentz force. This is nothing less than the conservation of canonical momentum. At high magnetic fields (11 and 14 T in Fig. 2) only a few electric subbands are seen at considerably higher voltage than in the low magnetic field case. At lower voltages new structure can be observed (denoted M_n) which also shifts to higher voltages upon further increase of the magnetic field. The emergence of these structures can already be observed at 8 T.

In order to understand these features we have calculated the energy levels of an electron near an electrically biased barrier by solving the Schrödinger equation numerically

$$\left[\frac{1}{2m^*} (\mathbf{p} - e\mathbf{A})^2 + V(z) \right] \psi(\mathbf{r}) = \epsilon \psi(\mathbf{r}). \quad (1)$$

Here, $\mathbf{A} = (0, -Bz, 0)$, i.e., the magnetic field is applied in the x direction. Equation (1) reduces to a one-dimensional differential equation in z . $V(z)$ is the potential containing contributions from the applied voltage, the first barrier and the accumulation region before the first barrier. The accumulation potential is modelled according to a variational solution.¹⁵ It should be noted that due to the weak

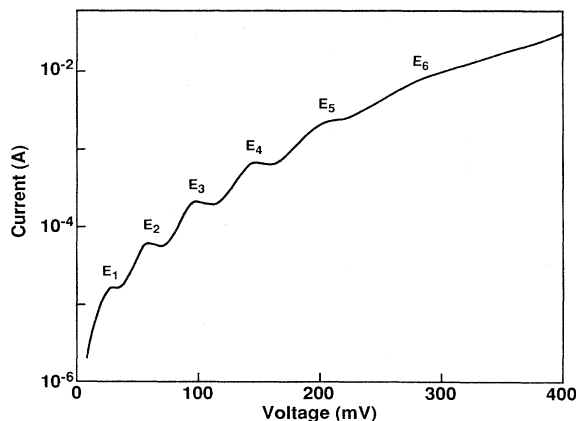


FIG. 1. Current-voltage characteristics of the structure at 6 K without an applied magnetic field. The electric subband number is indicated by E_n .

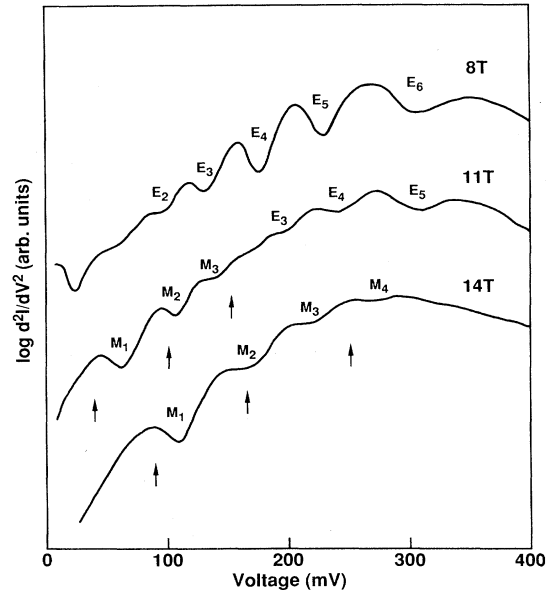


FIG. 2. d^2I/dV^2 vs voltage for magnetic fields of 8, 11, and 14 T. The curves are arbitrarily displaced in the vertical direction. E_n denotes the electric subbands and M_n the high magnetic field resonances. The arrows correspond to calculated values of M_n for $\epsilon_F = 20$ meV (see text).

binding energy of the bound state in the accumulation layer (typically around 5 meV, confirmed by a self-consistent calculation¹⁶), the behavior in a high transverse magnetic field is three rather than two dimensional. Figure 3 shows the assumed potential and the calculated energy levels for a magnetic field of 14 T and an electric field of 20 kV/cm, which corresponds to a bias voltage of 150 mV (taking

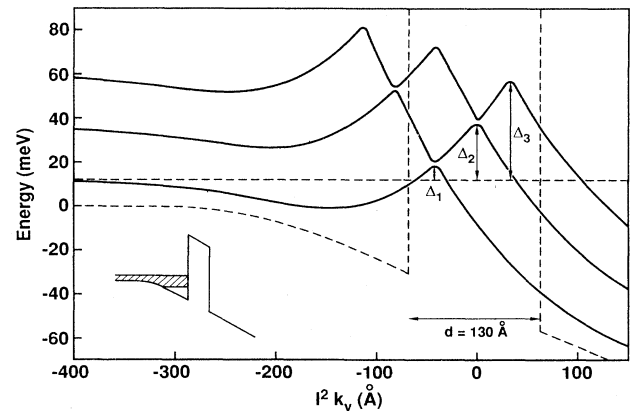


FIG. 3. The energy levels are plotted versus the orbit center of the wave function for $B = 14$ T and $E = 20$ kV/cm ($V = 150$ mV). The dashed lines represent the potential used in the calculation, and the bottom of the conduction band at the far left. The energy differences between this line and the anticrossings, Δ_n , are also shown. The gaps at the anticrossings have been exaggerated for clarity. The inset illustrates the situation schematically.

into account the voltage drop across the accumulation region and assuming a linear voltage drop through the remainder of the structure). The horizontal axis is $l^2 k_y$ ($l = \sqrt{\hbar/eB}$), which would be the "orbit center" of the wave functions in the absence of a barrier and an electric field. To the left of the barrier the energy drops slightly due to the influence of the accumulation potential, at the barrier it increases sharply, and to the right it follows the potential given by the electric field. As a consequence, the levels from the left- and right-hand side cross each other in the barrier, forming anticrossing states (the gap depends on the barrier parameters and is exaggerated in the figure). These states are the only ones contributing to tunneling, because their wave functions have a considerable probability amplitude on both sides of the barrier. When the electric field is increased, the anticrossing points are pulled down and shifted to the left. In a sweep of the bias voltage at constant magnetic field these anticrossing points successively drop below the Fermi energy in the emitter thus opening up new channels that contribute to conduction. Such a behavior should result in a change of the conductance and, therefore, lead to features in d^2I/dV^2 , whenever such a point crosses the Fermi energy. This is exactly what is observed in the present experiment. Accordingly, a strong transverse magnetic field induces internal structure in the tunneling barrier. We point out that these resonant features (we will call them "magnetic features") are qualitatively different from the low-magnetic-field resonances ("electric features"), which are caused by tunneling into a quasi-two-dimensional system. Similar features have been observed by Snell *et al.*¹⁰ in dI/dB vs B at constant bias for electrons tunneling into a three-dimensional system, and, very recently, by Alves *et al.*¹⁷ upon tunneling into a very wide quantum well. In

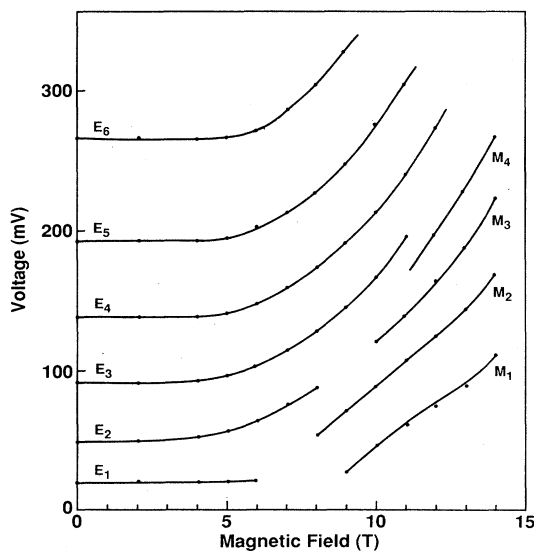


FIG. 4. Fan diagram (bias voltage vs magnetic field) of all observed minima in d^2I/dV^2 . The features originating from electric subbands are labeled E_n , the magnetic features M_n . The points are taken from the measurements, the lines are a guide for the eye.

both cases, however, the authors assumed the formation of a two-dimensional electron system on the injector side, which is only slightly perturbed by the magnetic field. They interpreted the oscillations as caused by tunneling of these two-dimensional electrons at the Fermi level into interface states. In contrast, we consider magnetic quantization important on both sides of the barrier, since in a high magnetic field the cyclotron energy readily exceeds the binding energy of the electrons in the accumulation layer.

So far, the argument has been qualitative. For a more detailed analysis we have plotted all the observed minima in d^2I/dV^2 in a fan diagram of voltage versus magnetic field in Fig. 4. The electric features are denoted E_n and the magnetic ones M_n , as in Fig. 2. The curves in Fig. 2 correspond to vertical cross sections through Fig. 4. We also investigated dI/dB as a function of B , which corresponds to horizontal sections of Fig. 4. This way of plotting the data reveals clear oscillations already in the first derivative, however the distinction between electric and magnetic features is not as easily made. To enable a detailed comparison between theory and experiment we calculated the "magnetic barrier height," Δ_n (i.e., the energy difference between the bottom of the conduction band to the far left of the barrier and the first three anticrossings in the barrier), as a function of the bias voltage for 11 and 14 T. The result is shown in Fig. 5. The crosses denote the calculated points, the lines are guides for the eye. As mentioned above, the resonances are interpreted to occur when the anticrossings drop below the Fermi level, ϵ_F . The Fermi energy in the bulk, to the left of the barrier, can now be used as a fit parameter. A reasonable fit is obtained by choosing $\epsilon_F = 20$ meV. The horizontal line in Fig. 5 corresponds to this choice. The intersections of this line with the Δ_n versus voltage curves define the bias voltage where the resonances M_n should occur. These values are indicated by arrows in Fig. 2 for the 11- and 14-T traces. The overall agreement is quite good. It enables us

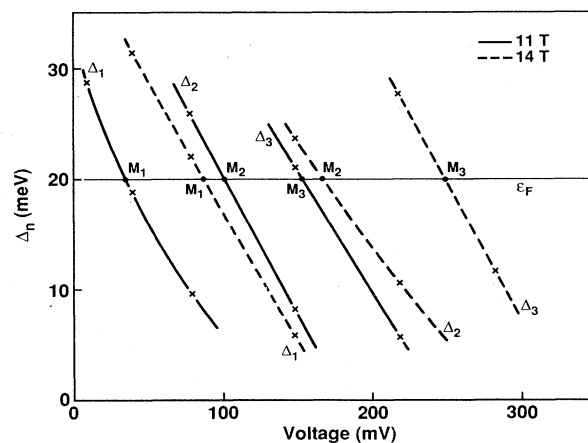


FIG. 5. The magnetic barrier heights, Δ_n , plotted vs bias voltage. The crosses are calculated points, the lines a guide for the eye. The horizontal line represents a Fermi energy of 20 meV; the crossing points M_n should be compared with the experiment (see arrows in Fig. 2).

to correctly reproduce the result that M_1 (14 T) occurs at lower voltage than M_2 (11 T), and M_3 (11 T) at lower voltage than M_2 (14 T). A Fermi energy of 20 meV is consistent with an electron density of $2 \times 10^{17} \text{ cm}^{-3}$, which is somewhat higher than the targeted concentration of $7 \times 10^{16} \text{ cm}^{-3}$. However, accurate control of impurity incorporation at this doping level is difficult in our OMCVD system. For a better fit of the data at higher bias it might become necessary to calculate the potential distribution through the whole structure self-consistently, including the magnetic field.

In conclusion, we have delineated two entirely different

regimes of resonant tunneling in a transverse magnetic field. In low magnetic fields, the current-voltage characteristics are dominated by tunneling into the two-dimensional density of states of the quantum well, while in high magnetic fields, the transport becomes diffusive and is governed by edge states bound to the first barrier.

We would like to thank S. J. Allen for useful and stimulating discussions and A. Zrenner for providing us with the results of a self-consistent calculation for the accumulation layer. One of us (F.M.P.) is supported by the Belgian National Science Foundation.

*Present address: University of Antwerp (UIA), Department of Physics, B-2610 Antwerp, Belgium.

- ¹L. L. Chang, L. Esaki, and R. Tsu, *Appl. Phys. Lett.* **24**, 593 (1974).
- ²S. Luryi, *Appl. Phys. Lett.* **47**, 490 (1985).
- ³B. Ricco and M. Ya. Azbel, *Phys. Rev. B* **29**, 1970 (1984).
- ⁴V. J. Goldman, D. C. Tsui, and J. E. Cunningham, *Phys. Rev. B* **35**, 9387 (1987).
- ⁵E. E. Mendez, L. Esaki, and W. I. Wang, *Phys. Rev. B* **33**, 2893 (1986).
- ⁶W. Zawadzki, *Semicond. Sci. Technol.* **2**, 550 (1987).
- ⁷P. Gueret, A. Baratoff, and E. Marclay, *Europhys. Lett.* **3**, 367 (1987).
- ⁸R. A. Davies, D. J. Newson, T. G. Powell, M. J. Kelly, and H. W. Myron, *Semicond. Sci. Technol.* **2**, 61 (1987).
- ⁹M. L. Leadbeater, L. Eaves, P. E. Simmonds, G. A. Toombs, F. W. Sheard, P. A. Claxton, G. Hill, and M. A. Pate, *Solid State Electron.* **31**, 707 (1988).
- ¹⁰B. R. Snell, K. S. Chan, F. W. Sheard, L. Eaves, G. A. Toombs, D. K. Maude, J. C. Portal, S. J. Bass, P. Claxton, G. Hill, and M. A. Pate, *Phys. Rev. Lett.* **59**, 2806 (1987).
- ¹¹K. S. Chan, L. Eaves, D. K. Maude, F. W. Sheard, B. R. Snell, G. A. Toombs, E. S. Alves, J. C. Portal, and S. Bass, *Solid State Electron.* **31**, 711 (1988).
- ¹²T. W. Hickmott, *Solid State Commun.* **63**, 371 (1987).
- ¹³L. Brey, G. Platero, and C. Tejedor, *Phys. Rev. B* **38**, 9649 (1988).
- ¹⁴F. Ancilotto, *J. Phys. C* **21**, 4657 (1988).
- ¹⁵F. Stern, *Phys. Rev. B* **15**, 4891 (1972).
- ¹⁶A. Zrenner (private communication).
- ¹⁷E. S. Alves, M. L. Leadbeater, L. Eaves, M. Henini, O. H. Hughes, A. Celeste, J. C. Portal, G. Hill, and M. A. Pate, *Fourth International Conference on Superlattices, Microstructures, and Microdevices, Trieste, Italy, 1988* [Superlattices Microstruct. (to be published)].